Applied Clay Science 51 (2011) 209–213

Contents lists available at ScienceDirect

Applied Clay Science

journal homepage: www.elsevier.com/locate/clay

Bentonite functionalized with propyl sulfonic acid groups used as catalyst in esterification reactions

D.S. Moraes [a,*], R.S. Angélica [c], C.E.F. Costa [b], G.N. Rocha Filho [b], J.R. Zamian [b]

[a] UFPA — Universidade Federal do Pará, Campus de Marabá, Faculdade de Engenharia de Minas e Meio Ambiente, 68505-080, Marabá, PA, Brazil
[b] UFPA — Universidade Federal do Pará, Instituto de Ciências Exatas e Naturais, Laboratório de Catálise e Oleoquímica, 66075-110, Belém, PA, Brazil
[c] UFPA — Universidade Federal do Pará, Instituto de Geociências, 66075-110 Belém, PA, Brazil

ARTICLE INFO

Article history:
Received 7 July 2010
Received in revised form 25 October 2010
Accepted 13 November 2010
Available online 29 November 2010

Keywords:
Bentonite
Functionalization
MTPS
Catalysts
Esterification

ABSTRACT

The main objective of this work is the functionalization of bentonite from the Amazon (region) by the grafting of propyl sulfonic acid groups to catalyze the esterification reaction of acetic acid and 1-propanol. Functionalization was accomplished by anchoring, oxidation and acid activation of (3-mercaptopropyl) trimethoxysilane, (MTPS). The procedure gave acid properties to the raw bentonite. This material, acting as a catalyst, increased the reaction speed and improved the yield by about 12% compared to the uncatalyzed reaction. The functionalized bentonite was characterized by XRD, TG/DTA, FTIR, N_2 adsorption/desorption at 77 K and XRF, and the surface acidity was determined by titration.

1. Introduction

The use of smectite in catalysis began in the mid-1930s when acidified montmorillonites were used as catalysts in petroleum cracking reactions (Occelli and Rennard, 1988; Pinnavaia, 1983; Thomas and Thomas, 1997). By the 1970s, the possibility of modification of these clay minerals by other processes, including the pillaring or intercalation of anions, complexes and organic compounds between layers of clay minerals, was discovered (Figueras, 1988; Vaugham, 1988). These modifications led to new material properties and reactivities that extended the applications of this group of clay minerals as catalysts (González et al., 1999; Sanabria et al., 2008; Swarnakar et al., 1996).

The most common method of transforming smectite into active materials for adsorption and catalysis involves treating raw bentonite with acidic solutions, leading to the formation of solids with sufficient acidity for use in processes (Laszlo, 1987, 1990; Sabu et al., 1999). These treatments include phenol alkylation (Kaplan, 1966), unsaturated hydrocarbon polymerization (Hojabri, 1971; Nijopwouo et al., 1987) and edible oil clarification (Morgan et al., 1985).

Due to the development of the field of nanotechnology, the study of the surface modification of clay minerals, mainly organoclays, has garnered attention because it generates versatile compounds with new potential application (Schoonheydt, 2002). These materials are relatively inexpensive and may be produced on large scales primarily because the basic ingredient used in production is readily available from natural sources (Paiva et al., 2008). These reasons demonstrate the immense potential of these materials that sparked interest in their application in catalysis.

The main purpose of this study is the functionalization of a bentonite from the Amazon region with propyl sulfonic groups obtained by the oxidation and acidification of previously anchored (3-mercaptopropyl)trimethoxysilane. The organobentonite will be used to catalyze the esterification of acetic acid with 1-propanol. This work intends to demonstrate the preparation of special materials from local materials, extending beyond the traditional forms of mineral exploitation common in the region.

2. Experimental

2.1. Catalyst preparation

The main clay mineral of the bentonite used in this work is a montmorillonite with a high iron content and structural formula $K_{0,33}Ca_{0,05}Na_{0,03}(Al_{1,34}Mg_{0,41}Fe_{0,26}Ti_{0,03})[(OH)_2/Al_{0,19}Si_{3,81}O_{10}]$, collected from a site northeast of Balsas, south of Maranhão State, Brazil (Moraes et al., 2010). The clay fraction (particle size <2 μm) of the collected material, called Balsas Clay, was separated from sand and silt. This concentration was carried out by the successive grinding and separation of the particles in deionized water using ultrasonic disaggregation for 5 min. The dispersions were passed through a 0.062-mm sieve. The <2-μm clay fraction was obtained by

* Corresponding author. Tel./fax: +55 91 32499780.
E-mail address: dorsan@ufpa.br (D.S. Moraes).

0169-1317 © 2010 Elsevier B.V. Open access under the Elsevier OA license.
doi:10.1016/j.clay.2010.11.018

gravitational sedimentation of the purified samples, and the <0.2-μm fraction was obtained by the centrifugal sedimentation of the <2-μm dispersion in a constant temperature centrifuge at 30 °C according to a modified procedure from Tributh and Lagaly (1986). The composition determined by inductively coupled plasma-optical emission spectrometry (ICP-OES) (wt.%) was SiO_2, 51.11; Al_2O_3, 17.43; Fe_2O_3, 6.33; Na_2O, 0.11; K_2O, 4.33; MgO, 3.91; CaO, 0.78; P_2O_5, 0.09; TiO_2, 0.56 and MnO, 0.02. Furthermore, the loss on ignition was 14.8%, the specific surface area (S_{BET}) was 68.5 $m^2 g^{-1}$, the microporous area ($Micro S_{DeBoer}$) was 51.9 $m^2 g^{-1}$, the total pore volume (PV_{BJH}) was 0.020 cm^3 g^{-1}, and the cation exchange capacity (CEC) was 105.4 meq per 100 g of bentonite (Moraes et al., 2010).

The grafting agent, (3-mercaptopropyl)trimethoxysilane (MTPS, $(HS(CH_2)_3)Si(OCH_3)_3$), of 95% purity, was purchased from Sigma-Aldrich and used without further purification. Toluene P.A., used as a solvent for the functionalizing agent and bentonite dispersing, was purchased from Synth. Ethyl ether P.A. (Synth) and dichloromethane P.A. (Merck) were used to extract the functionalizing agent excess. H_2O_2 (35%) and ethanol P.A. (Nuclear) and H_2SO_4 P.A. (Merck) were used in the oxidation and acid activation of anchored MTPS. The KCl and KOH solutions used in the acidity measurements were prepared with reagent grade chemicals from Fluka and Nuclear, respectively. All solutions were prepared with deionized water.

Bentonite functionalization was performed according to the procedure for functionalization of ordered mesoporous materials reported in Bossaert et al. (1999) and Rác et al. (2006, 2007). Five grams of dry bentonite was dispersed in a MTPS solution (10 g) in dry toluene (250 mL, treated with a 3 Å molecular sieve for 24 h) at 383 K for 24 h. The dispersion was stirred for 8 h and then refluxed for 24 h. The collected solid was purified in a Soxhlet extractor with a mixture of CH_2Cl_2/Et_2O (50 mL each) for 24 h and air-dried. This synthesis intermediate will henceforth be called bentonite-SH. Anchored thiol groups were oxidized with H_2O_2 (10.2 mL)/MeOH (24.4 mL) for 24 h. The dispersion was filtered, rinsed with H_2O/EtOH (50 mL each) and redispersed in 0.1 M H_2SO_4 for another 4 h. Finally, the material was rinsed with deionized H_2O until neutral pH was reached, dried at 333 K and stored in a desiccator for further characterization. The oxidized and acidified functionalized material will henceforth be called bentonite-SO_3H.

An equal amount of the clay fraction (5 g) was also subjected to the acid activation that was performed on the functionalized material to investigate only the effects caused by this treatment in the raw bentonite.

2.2. Characterization

The raw and functionalized bentonite samples were characterized by powder X-ray diffractometry (XRD). XRD patterns were obtained for oriented samples with a Panalytical X'PERT PRO MPD (PW3040/60) diffractometer with a ceramic X-ray tube (λ CuKα1 = 1.540598 Å). The following analysis conditions were used: 40 kV voltage, 30 mA current, 3–35° scan range, 0.016° step size, continuous scan mode, and 99.7 s counting time. The oriented samples were prepared by first dispersing the bentonite in deionized water. Using a pipette, the dispersions were then placed onto glass slides and dried overnight under atmospheric conditions at room temperature (Wolters et al., 2009).

Thermal studies of the samples (TG/DTA) were carried out using a thermal science thermoanalyzer, model PL-STA. Samples were tested in a N_2 atmosphere (50 mL/min) using alumina crucibles, a 298–1273 K temperature range and a 10 K min^{-1} heating rate.

Fourier transform infrared spectrometry (FTIR) analysis was carried out using a Perkin Elmer 1760 X FTIR spectrometer in the 4000–400 cm^{-1} region.

The specific surface area (total SA), micropore area (micro SA), pore volume (total PV) and pore size distributions of the samples were determined by nitrogen adsorption/desorption analysis at 77 K using a quantachrome analyzer, model NOVA 1200. The results were plotted by BET (Brunauer–Emmett–Teller), De Boer and BJH (Barrett–Joyner–Halenda) methods, respectively.

A Shimadzu, EDX-700 model X-ray fluorescence by dispersive energy spectrophotometer (XRF) was used to determine the sulfur content and indirectly quantify the propyl sulfonic groups on the material surface because each MTPS carbon chain contains one sulfur atom. The analysis was carried out in a He atmosphere.

The surface acidity was determined using acid–base titration as described by Rác et al. (2006, 2007). In a typical measurement, 0.5 g of the solid was dispersed in 50 mL of 0.1 M KCl. The dispersion was stirred for 20 min and titrated with 0.2 M KOH in the presence of phenolphthalein.

2.3. Catalytic testing and product characterization

The esterification reaction was carried out by mixing 2.3 g of the dried bentonite-SO_3H, 30 mL (524 mmol) of acetic acid and 39.5 mL (524 mmol) 1-propanol in a 250-mL round bottom flask equipped with a reflux condenser at 373 K. The system was sealed to prevent leakage. After every 2 h, a 0.5-g aliquot of the reactional mixture was removed to evaluate the reactant conversion by measuring the total solution acidity. Analyte aliquots were titrated with 0.2 M KOH in the presence of phenolphthalein (AOCS Method Cd 3d-63, 2003). After 25 h of reaction, the catalyst was recovered by filtration, rinsed with methanol and dried at 333 K. The product was isolated by extracting the polar phase (reactants) with deionized water and subsequent product separation (ester).

Products were identified by gas chromatography coupled to a mass spectrometer (GC/MS/MS) using a Varian GC Plus Varian Saturn 2100T MS/MS, FTIR using a thermo electron corporation IR 100 in the 400–4000 cm^{-1} range and ^1H and ^{13}C nuclear magnetic resonance (NMR) using a Varian Gemini 300 spectrometer at 300 and 75 MHz, respectively.

3. Results and discussion

X-ray diffraction patterns of raw and functionalized bentonite (Fig. 1) showed characteristic reflections of montmorillonite, illite and quartz (Moraes et al., 2010). After anchoring, a shift of the characteristic reflection of montmorillonite at 2θ = 5.95° (d_{001} = 14.85 Å) to 2θ = 6.03° (d_{001} = 14.62 Å) was observed. This result indicates that the montmorillonite experienced the anchor process (bentonite-SH diffractograms not shown), and the other clay minerals were unaffected by this process. Functionalization of the bentonite involves the direct condensation reaction between the terminal –OH groups from the silicate surface with alkoxy silane groups of the

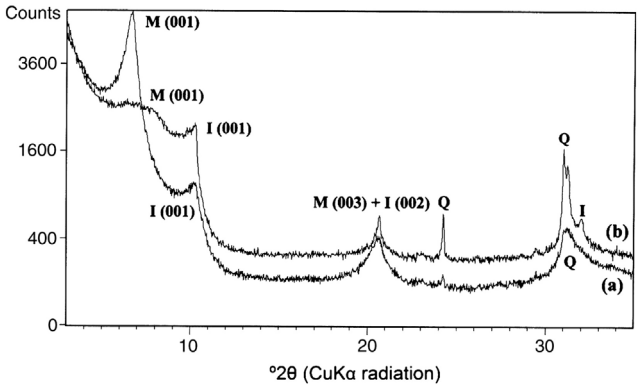

Fig. 1. X-ray diffractogram of the (a) raw bentonite and (b) bentonite-SO_3H samples. I: illite, M: montmorillonite, Q: quartz.

grafting agent. In this step, the MTPS hydrolysable methoxy groups ($-OCH_3$) were desorbed as methanol during the coupling reactions. The propylene group acts as a link between the silicon atom and the thiol group (Guimarães et al., 2009). The oxidation and acidification of the bentonite-SH shifted the main montmorillonite reflection to $2\theta = 6.17°$ ($d_{001} = 14.30$ Å), which caused a larger crystallinity loss. This loss was due to the acid treatment employed after the bentonite-SH oxidation because this treatment can remove aluminum ions from the clay mineral, explaining, at least in part, the crystallinity loss (Rodríguez et al., 2007).

To corroborate this theory of increasing structural disorder, the raw bentonite was subjected to the same acid treatment used in the activation of the thiol groups. It presented the same characteristics as the investigated sample, as shown in Fig. 1, i.e., a broadening and decreasing in relative intensity.

The infrared spectra for raw and functionalized bentonite (Fig. 2) showed two bands at 3424 and 1635 cm^{-1} attributed to the stretching vibration and corresponding angular deformation band, respectively, from the presence of physisorbed water (Pan et al., 2008). The strong band occurring around 3627 cm^{-1} is attributed to the stretching vibration of the Mg–OH, Al–OH or Fe–OH structural hydroxyls groups, typical of montmorillonite (Wolters and Emmerich, 2007). The other vibrational modes characteristic of this clay mineral are the broad band at 1032 cm^{-1} assigned to Si–O stretching vibrations of the Si–O–Si tetrahedron, the band around 516 cm^{-1} assigned to the angular deformation of Si–O–Al and the band centered at 470 cm^{-1} assigned to the angular deformation of Si–O–Si (Pan et al., 2008).

The presence of propyl sulfonic groups can be characterized by the stretching vibrations of methylene groups (–CH_2–) occurring in the 3000–2800 cm^{-1} region. The aliphatic CH_2 groups give rise to a doublet at 2929 and 2847 cm^{-1}, assigned to the asymmetric and symmetric stretches, respectively. In low energy regions, the vibrations of these functional groups are masked by the bentonite vibrational modes. For example, the angular deformation vibrations of –CH_2– groups that should be observed at about 1460 cm^{-1} (and have lower intensity than those of stretching) are masked by the broad band coming from the Si–O stretching vibrations of the Si–O–Si tetrahedron from the support material. To confirm the formation of the sulfonic acid species, a careful analysis was performed and revealed that the magnified bands at 1397 and 1417 cm^{-1} (Fig. 3) are only found in sample with –SO_3H groups anchored due to the asymmetric stretching of SO_2 moieties, confirming the oxidation of the MTPS groups. These values are virtually identical to those found in the literature (Rác et al., 2006).

The TG curves of both materials (Fig. 4) show a mass loss of approximately 2% between 30 and 120 °C, which may be attributed to the water that is adsorbed onto the external surface and/or between clay mineral layers and to the water coordinated to interlayer cations (Guggenheim and Koster van Groos, 2001; Wolters and Emmerich, 2007).

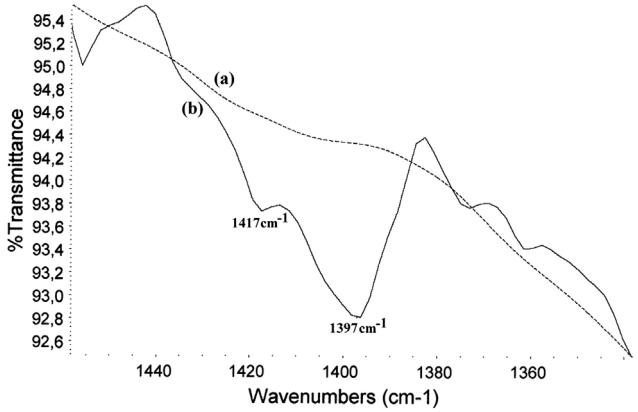

Fig. 3. FTIR spectra of the (a) raw bentonite and (b) bentonite-SO_3H samples in the 1460–1340 cm^{-1} region.

The second mass loss in raw bentonite (approximately 4.5%) that occurred between 400 and 600 °C can most likely be attributed to the dehydroxylation of smectite with high iron content (Brigatti, 1983). The functionalized bentonite had an additional weight loss (about 6.7%) that occurred almost immediately. This is attributed to the combination of dehydroxylation and the decomposition of the grafted alkyl sulfonic groups because organic matter decomposition in a N_2 atmosphere characteristically occurs between 300 and 600 °C. A similar situation was recently reported in functionalized clays with organic groups (Guimarães et al., 2009).

The DTA curve peaks (Fig. 4) associated with the first two mass loss processes corroborate the proposed assignments of the water loss, dehydroxylation reactions and organic matter decomposition reactions under an inert atmosphere because these processes are typically endothermic. The third endothermic peak (a = 873 °C, b = 880 °C) is not associated with mass loss, indicating a possible structural rearrangement (Moraes et al., 2010; Wolters and Emmerich, 2007).

The N_2 adsorption/desorption isotherms for raw samples present a profile that is distinctive from the functionalized sample isotherms. The raw material has a type II IUPAC classification profile, which is common in smectites (Abdellah Elm'chaouri and Simonot-Grange, 1999). The functionalized material exhibits a step-shaped isotherm indicative of the pore-filling step (Rác et al., 2006). Table 1 summarizes some of the physical properties of the functionalized and raw material. In the functionalized material, the specific surface

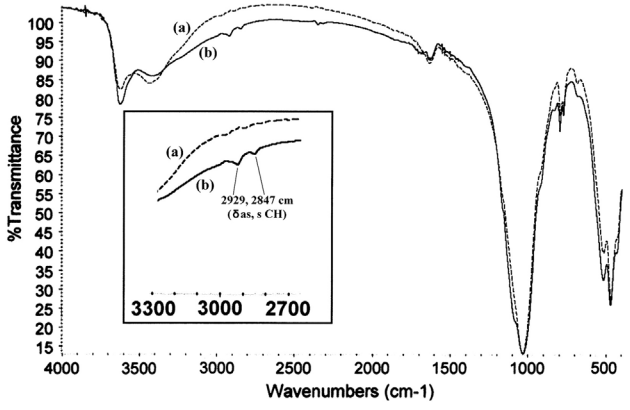

Fig. 2. FTIR spectra of the (a) raw bentonite and (b) bentonite-SO_3H samples.

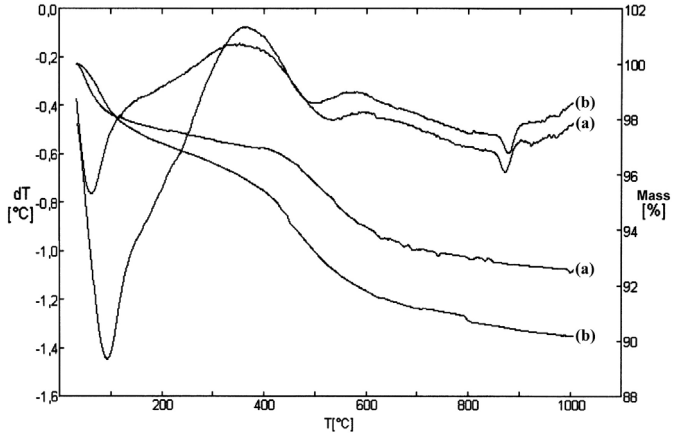

Fig. 4. TG/DTA curves of the (a) raw bentonite and (b) bentonite-SO_3H samples.

Table 1
Comparison of effects of functionalization on some physical properties of raw bentonite.

Catalyst	S_{BET} ($m^2 g^{-1}$)	$Micro S_{De\ Boer}$ ($m^2 g^{-1}$)	$Dp_{(average)}$ Å	Vp_{BJH} ($cm^3 g^{-1}$)
Raw bentonite	68	52	34	0.02
Acidified bentonite	96	42	26	0.08
Bentonite-SO_3H	31	8	38	0.04

Table 2
Acidity and sulfur content of catalyst.

Catalyst	Acidity (mmol $H^+ g^{-1}$)	S content (wt.%)
Raw bentonite	0	0
Acidified bentonite	0.24	0
Bentonite-SO_3H	0.5	0.7

area (S_{BET}) is smaller than that of the raw material. This area reduction is attributed to the occupation or even blocking some bentonite pores by the grafting agent, which may explain the microporous area reduction ($Micro S_{De\ Boer}$). The average pore diameter, pore volume and pore size distribution were calculated by the BJH method. Though this model systematically underestimates the pore size, it shows some of the functionalization effects in the textural properties of clay mineral.

The increase in the average pore diameter is attributed in part to the reduced contribution from micropores, shown in Fig. 5. After functionalization, almost no pores with diameters below 30 Å are detected. However, the acid treatment applied after the anchoring of MTPS groups (bentonite-SH) can increase both the total pore volume (Vp) and the average pore diameter (Dp). In this treatment, the original interlayer cations were replaced by the protons of the acid without leaching significant amounts of aluminum from the clay mineral structure, increasing these parameters (Guimarães et al., 2009).

The results from the acidity analysis and sulfur content in raw and functionalized samples are presented in Table 2. The amount of sulfur present in the functionalized sample is correlated with the amount of grafting agent determined to the bentonite structure. The acidity measured is also indicative of the anchoring success, oxidation and acid activation of MTPS groups to the structure of the bentonite support. To strengthen this proposition the acidity of the raw bentonite submitted only to the process of acid treatment used to acidify the MTPS groups (0.1 M H_2SO_4 for 4 h) was measured. The value found is about half the value obtained for the functionalized material (Table 2).

Although the main physical property values of functionalized bentonite in this work are less than those of other materials that underwent similar functionalization processes, such as MCMs and SBA-15 (Rác et al., 2006, 2007), their acidities are roughly the same. Thus, the produced material has all the properties required for catalyzing organic reactions in which Bronsted acidity is required.

3.1. Catalytic testing

The catalyst performance of bentonite-SO_3H was evaluated in the esterification reaction between acetic acid and 1-propanol and is summarized in Fig. 6. The conversion for the catalyzed reaction with bentonite-SO_3H was around 65%. Without the catalyst, the reaction yield was around 53%, and the yield was around 57% using acid bentonite. Based on these results, the most effective catalyst is the functionalized bentonite because it has the largest shift from equilibrium relative to the absence of the catalyst, highlighting the importance of the anchored propyl sulfonic acid groups. Under the experimental conditions used here, the equilibrium was reached after approximately 10 h with bentonite-SO_3H, while the non-catalyzed process takes around 20 h. Finally, the reaction speed for the first 2 h is significantly greater when using bentonite-SO_3H.

4. Conclusions

Based on the results presented in this paper, the following conclusions can be drawn:

1. The catalyst synthesis was successful, significantly increasing the acidity of the starting material.
2. The results of catalytic tests indicate the importance of anchoring the MTPS groups given that the derivative catalyst was the most effective in the esterification reaction between acetic acid and 1-propanol.
3. The new equilibrium state for the catalyzed reaction is achieved much faster than in the uncatalyzed reaction.
4. The bentonite clay studied here is a promising alternative support material for catalyst preparation because, as a natural resource, it does not require synthesis processes, which can be quite expensive.
5. This work creates new possibilities for the use of bentonite functionalized with organic groups as catalysts in other organic reactions.

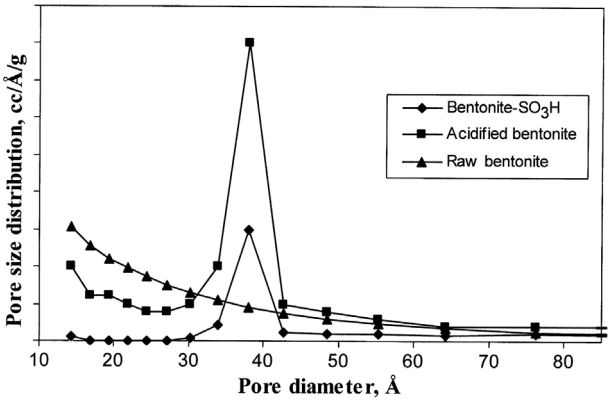

Fig. 5. Pore size distributions of the (a) raw bentonite, (b) bentonite-SO_3H and (c) acidified bentonite samples.

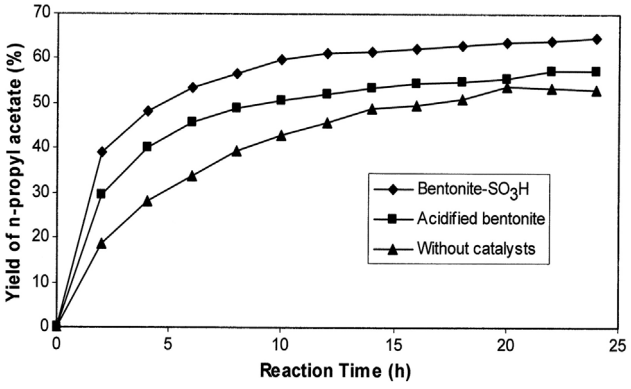

Fig. 6. Catalytic performance of functionalized and acidified bentonite at 373 K.

References

Abdellah Elm'chaouri, Simonot-Grange, M., 1999. Données expérimentales et modélisation dádsorption des systémes N_2(g)/montmorillonite potassique de Camp-Berteau et N_2(g)/hydrotalcite Carbonatée. Thermochimica Acta 339, 117–123.

AOCS Official Method Cd 3d-63, Acid Value, Revised 2003.

Bossaert, W.D., De Vos, D.E., Van Rhijn, W.M., Bullen, J., Grobet, P.J., Jacobs, P.A., 1999. Mesoporous sulfonic acid as selective heterogeneous catalysts for the synthesis of monoglycerides. Journal of Catalysis 182, 156–164.

Brigatti, M.F., 1983. Relationship between composition and structure in Fe-rich smectites. Clay Minerals 18, 177–186.

Figueras, F., 1988. Pillared clays as catalysts. Catalysis Reviews — Science and Engineering 30, 457–499.

González, F., Pesquera, C., Benito, I., Herrero, E., Pocio, C., Casuscelli, S., 1999. Pillared clays: catalytic evaluation in heavy oil cracking using a microactivity test. Applied Catalysis A: General 181, 71–76.

Guggenheim, S., Koster van Groos, A.F., 2001. Baseline studies of the clay minerals society source clays: thermal analysis. Clays and Clay Minerals 49 (5), 433–443.

Guimarães, A.M.F., Ciminelli, V.S.T., Vasconcelos, W.L., 2009. Smectite organofunctionalized with thiol groups for adsorption of heavy metal íons. Applied Clay Science 42, 410–414.

Hojabri, F., 1971. Gas-phase catalytic alkylation of aromatic hydrocarbons. J. Appl. Chem. Biotechnol 21, 87–89.

Kaplan, H., 1966. US Patent 3287422 4.

Laszlo, P., 1987. Chemical reaction on clays. Science 235, 1473–1477.

Laszlo, P., 1990. Catalysis of organic reactions by inorganic solids. Pure & Appl. Chem. 62, 2027–2030.

Moraes, D.S., Angélica, R.S., Costa, C.E.F., Rocha Filho, G.N., Zamian, J.R., 2010. Mineralogy and chemistry of a new bentonite occurrence in the Eastern Amazon region, Northern Brazil. Applied Clay Science 48, 475–480.

Morgan, D.A., Shaw, D.B., Sidedbottom, M.J., Soon, T.C., Taylor, R.S., 1985. The function of bleaching earths on the processing of palm, palm kernel and coconut oils. J. Am. Oil Soc. 62, 292–299.

Nijopwouo, D., Roques, G., Wandji, R.A., 1987. A contribution to the study of the catalytic action of clays on the polymerization of styrene: characterization of polystyrene. Clay Miner. 22, 145–156.

Occelli, M.L., Rennard, R.J., 1988. Hydrotreating catalysts containing pillared clays. Catalysis Today 2, 309–319.

Paiva, L.B., Morales, A.R., Valenzuela-Diaz, F.R., 2008. Organoclays: properties, preparation and applications. Applied Clay Science 42, 8–24.

Pan, J., Wang, C., Guo, S., Li, J., Yang, Z., 2008. Cu supported over Al-pillared interlayer clays catalysts for direct hydroxylation of benzene to phenol. Catalysis Communication 9, 176–181.

Pinnavaia, T.J., 1983. Intercalated clay catalysts. Science 220, 365–371.

Rác, B., Molnár, Á., Fogo, P., Mohai, M., Bertóti, I., 2006. A comparative study of solid sulfonic acid catalysts based on various ordered mesoporous silica materials. Journal of Molecular Catalysis A: Chemical 244, 46–57.

Rác, B., Nagy, M., Pálinkó, I., Molnár, Á., 2007. Application of sulfonic acid functionalized MCM-41 materials-selectivity changes in various probe reactions. Applied Catalysis A: General 316, 152–159.

Rodríguez, Y.M.V., Beltrán, H.I., Vázquez-Labastida, E., Linares-López, C., Salmón, M., 2007. Synthesis and characterization of montmorillonite clays with modulable porosity induced with acids and superacids. Journal of Materials Research 22 (3), 788–800.

Sabu, K.R., Sakumar, R., Rekha, R., Lalithambika, M., 1999. A comparative study on H_2SO_4, HNO_3 and $HClO_4$ treated metakaolinite of a natural kaolinite as Friedel–Crafts alkylation catalyst. Catalysis Today 49, 321–326.

Sanabria, N., Álvarez, A., Molina, R., Moreno, S., 2008. Synthesis of pillared bentonite starting from the Al–Fe polymeric precursors in solid state, and its catalytic evaluation in the phenol oxidation reaction. Catalysis Today 133–135, 530–533.

Schoonheydt, R.A., 2002. Smectite-type clay minerals as nanomaterials. Clays and Clay Minerals 50 (4), 411–420.

Swarnakar, R., Brandt, K.B., Kydd, R.A., 1996. Catalytic activity of Ti- and Al-pillared montmorillonite and beidellite for cumene cracking and hydrocracking. Applied Catalysis A: General 142, 61–71.

Thomas, J.M., Thomas, W.J., 1997. Principles and Practice of Heterogeneous Catalysis. VHC Publishers Inc., New York.

Tributh, H., Lagaly, G.A., 1986. Aufbereitung und Identifizierung von Boden — und Lagerstättentonen. II. Korngrößenanalyse und Gewinnung der Tonsubfraktion In GIT Fachzeitschrift für das Laboratorium 30, 771–776.

Vaugham, D.E.W., 1988. Pillared clays — a historical perspective. Catalysis Today 2, 187–198.

Wolters, F., Emmerich, K., 2007. Thermal reactions of smectites — relation of dehydroxylation temperature to octahedral structure. Thermochimica Acta 462, 80–88.

Wolters, F., Legaly, G., Kahr, G., Nueesch, R., Emmerich, K., 2009. A comprehensive characterization of dioctahedral smectites. Clays and Clay Minerals 57 (1), 115–133.